Role of Arginine Residues in the Active Site of the Membrane-Bound Lytic Transglycosylase B from *Pseudomonas aeruginosa*†

Christopher W. Reid,‡ Neil T. Blackburn,§,¶ and Anthony J. Clarke*,‡,§

Guelph Waterloo Center for Graduate Work in Chemistry and Biochemistry and Department of Molecular and Cellular Biology, University of Guelph, Guelph, Ontario N1G 2W1, Canada

Received November 16, 2005; Revised Manuscript Received December 16, 2005

ABSTRACT: Lytic transglycosylases cleave the β-(1→4)-glycosidic bond in the bacterial cell wall heteropolymer peptidoglycan between the *N*-acetylmuramic acid (MurNAc) and *N*-acetylglucosamine (GlcNAc) residues with the concomitant formation of a 1,6-anhydromuramoyl residue. On the basis of both sequence alignments with and structural considerations of soluble lytic transglycosylase Slt35 from *Escherichia coli*, four residues were predicted to be involved in substrate binding at the −1 subsite in the soluble derivative of *Pseudomonas aeruginosa* membrane-bound lytic transglycosylase MltB. These residues were targeted for site-specific replacement, and the effect on substrate binding and catalysis was determined. The residues Arg187 and Arg188, believed to be involved in binding the stem peptide on MurNAc, were shown to play an important role in substrate binding, as evidenced by peptidoglycan affinity assays and SUPREX analysis using MurNAc-dipeptide as ligand. The Michaelis−Menten parameters were determined for the respective mutants using insoluble peptidoglycan as substrate. In addition to affecting the steady-state binding of ligand to enzyme, as indicated by increases in K_M values, significant decreases in k_{cat} values suggested that replacement of either Arg187 and Arg188 with alanine perturbed the stabilization of both the transition state(s) and reaction intermediate. Thus, it appears that Arg187 and Arg188 are vital for proper orientation of the substrate in the active site, and furthermore this supports the proposed role of the stem peptide at binding subsite −2 in catalysis. Replacement of Gln100, a residue that would appear to interact with the *N*-acetyl group on MurNAc, did not show any changes in substrate affinity or activity.

Bacteria possess an exoskeleton called peptidoglycan (or murein) which is used to withstand the strong turgor pressure exerted on their cytoplasmic membranes. This covalent structure is composed of two alternating aminosugars, *N*-acetylmuramic acid (MurNAc) and *N*-acetylglucosamine (GlcNAc),[1] which are joined by β-(1→4)-glycosidic linkages (Figure 1). The glycan strands are interconnected by short stem peptides which are attached to the lactyl moiety of muramic acid. This cross-linking generates a three-dimensional peptidoglycan sacculus of carbohydrate and amino acids that surrounds bacteria.

The generally accepted model for the biosynthesis of peptidoglycan in *Escherichia coli* invokes enzyme complexes comprised of both transferases, a collection of penicillin-binding proteins (PBPs), and the lytic transglycosylases (LTs) (reviewed in ref *1*). The high-molecular weight PBPs catalyze the incorporation of the newly synthesized and translocated peptidoglycan precursor molecule, lipid II, into the existing sacculus at sites made available through the action of LTs (*2*, *3*). While much effort has been made to understand the function and mechanism of action of the PBPs, the LTs have attracted considerably less attention.

The LTs are a class of bacterial autolysin that function to cleave peptidoglycan at the same site as lysozymes (EC 3.2.1.17; peptidoglycan *N*-acetylmuramoyl hydrolase), specifically the β-(1→4)-glycosidic bond between the MurNAc and GlcNAc residues. However, LTs are catalytically distinct from the hydrolytic lysozymes because they cleave peptidoglycan with the concomitant formation of 1,6-anhydro-MurNAc residues (*4*) (Figure 1). These enzymes are assumed to contribute to the metabolism of peptidoglycan, but their exact role has not been determined. They have been implicated as space makers for the insertion of new peptidoglycan into the cell wall during peptidoglycan remodeling and cell growth and as cell wall "zippers" during cell division

† This research was supported by an operating grant (MOP 49623) to A.J.C. from the Canadian Institutes of Health Research and a post-graduate scholarship (PGSB) to N.T.B. from the Natural Sciences and Engineering Research Council of Canada.

* To whom correspondence should be addressed. E-mail: aclarke@uoguelph.ca. Telephone: (519) 824-4120. Fax: (519) 837-1802.

‡ Guelph-Waterloo Centre for Graduate Work in Chemistry and Biochemistry.

§ Department of Molecular and Cellular Biology.

¶ Current address: Dade Behring Inc., 700 GBC Dr., Newark, DE 19714.

[1] Abbreviations used: GlcNAc, *N*-acetylglucosamine; GlcNAcMurNAc dipeptide, *N*-acetylglucosamine, β-(1→4)-*N*-acetylmuramyl L-alanine-L-isoglutamine; GdmCl, guanidinium chloride; H/D, hydrogen/deuterium; LT, lytic transglycosylase; MALDI, matrix-assisted laser desorption/ionization; MltB, membrane-bound lytic transglycosylase B; Mur, muramic acid; MurNAc, *N*-acetylmuramic acid; PBP, penicillin binding protein; SA, sinapinic acid; sMltB, soluble derivative of membrane-bound lytic transglycosylase B; SUPREX, stability of unpurified proteins from rates of H/D exchange; TOF, time-of-flight.

10.1021/bi052342t CCC: $33.50
Published on Web 01/31/2006

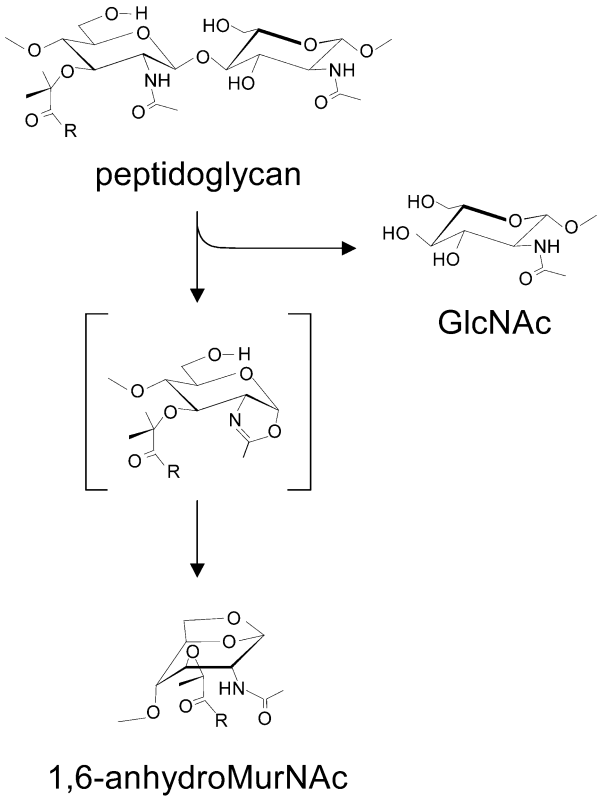

FIGURE 1: Structure of peptidoglycan and mode of action of lytic transglycosylases. The lytic transglycosylases catalyze the cleavage of peptidoglycan at muramoyl residues with the initial formation of an oxazolium intermediate and the subsequent formation of a terminal 1,6-anhydromuramoyl residue.

(*5*, *6*). LTs have been found associated with macromolecular transport systems such as type II secretion and the type IV pilus assembly systems (reviewed in ref *7*). They may also function in the recycling of old wall material and perhaps in the formation of pores to allow transport of DNA and proteins across the cell wall (*5*, *6*, *8*). The released 1,6-anhydromuropeptide products of the LTs are also involved in the pathobiology of bacterial infections (*9*−*11*).

LTs appear to be ubiquitous in the eubacteria that produce peptidoglycan (viz. all but the cell wall-less mycoplasmas) (*12*). Given their importance in bacterial function and in the pathobiology of bacterial infection, LTs would make an interesting candidate for new antimicrobial development. The known and hypothetical LTs have been organized into four families on the basis of differences within consensus signature sequences around their putative core catalytic domains (*12*). *Pseudomonas aeruginosa*, a Gram-negative, human opportunistic pathogen often associated with morbidity and mortality among cystic fibrosis patients (*13*), produces four family 3 LTs (*12*).

Our laboratory has been engaged in the biochemical characterization of LTs from Gram-negative organisms and in particular *P. aeruginosa*. We have previously provided a kinetic characterization and the first report of substrate affinity for this class of enzyme (*14*, *15*). Work with the β-hexosaminidase inhibitor NAG-thiazoline (*16*) provided the first evidence that the LT mechanism may employ substrate-assisted catalysis (*17*, *18*). Herein, we further our characterization of a soluble derivative of the family 3 LT MltB (termed sMltB) from *P. aeruginosa* by investigating the role of several residues predicted to exist at the −1 subsite of sMltB and participate in substrate binding.

EXPERIMENTAL PROCEDURES

Chemical Reagents and Enzymes. Complete EDTA-free protease inhibitor tablets, glycine, and isopropyl-α-D-thiogalactoside (IPTG) were purchased from Roche Molecular Biochemicals (Laval, PQ, Canada), while Ni-NTA resin was acquired from Qiagen (Valencia, CA). The BCA protein assay kit was obtained from Sigma Chemical Co. (St. Louis, MO). Source 15S column was supplied by Pharmacia Biotech (Baie d'Urf, PQ, Canada). All other chemicals were supplied by either Sigma Chemical Co. or Fisher Scientific (Nepean, ON, Canada) and were of reagent grade or HPLC grade where appropriate.

Insoluble peptidoglycan was isolated and purified from *P. aeruginosa* PA01 as previously described (*19*). The isolated peptidoglycan was treated with DNase, RNase, and Pronase and re-isolated by centrifugation as described by Glauner (*20*).

Bacterial Strains, Plasmids, and Growth Conditions. Bacterial strains and plasmids used and created in this study are summarized in Table 1. Cultures were routinely grown in Luria-Bertani (LB; 1% tryptone peptone, 1% NaCl, and 0.5% yeast extract) broth or LB agar plates at 37 °C. For protein expression experiments, cells were grown in Super Broth (3.2% tryptone peptone, 0.5% NaCl, and 2% yeast extract) at both 15 and 37 °C as appropriate. When necessary, growth media were supplemented with antibiotics at the following concentrations: kanamycin (Km; 30 μg/mL) or chloramphenicol (Cam; 34 μg/mL).

Site-Directed Mutagenesis. The Quick-Change site-directed mutagenesis system (Stratagene, LaJolla, CA) was used to create single amino acid replacements within sMltB. Conditions for the mutagenesis polymerase chain reaction (PCR) were those suggested by the manufacturer using PfuTurbo DNA polymerase. Plasmid pNBAC54-1 was used as template in a PCR using the following primers: Arg187→Ala, 5′-CTGTCCTTCTCCTACCCTgcCCCGCGCGGATTCTTC-AGC-3′ and 5′-GCTGAAGAATTCcgCGGGGCGGGTAG-GAGAAGGACAG-3′; Arg188→Ala, 5′-TCCTACCCT-CGCgcCGCGGAGTTCTTCAGCGGC-3′ and 5′-GCCGC-TGAAGAACTCCGCGgcGCGAGGGTAGGA-3′; Arg187 →Ala/Arg188→Ala, 5′-CCTTCTCCTACCCTgcCgcCGCG-GAGTTCTTCAGCGGC-3′ and 5′-GCCGCTGAAGAACT-CCGCGgcGgcAGGGTAGGAGAAGG-3′; Gln100→Ala, 5′-CGCCTGATGGACCCGGgcAGCCCCGACCTATACCCCA-3′ and 5′-GGGTATAGGTCGGGGCTGCCcgGTCCATCA-GGC-3′, with the changed nucleotides denoted by lowercase type. After PCR, the wild-type (wt) plasmid was digested with Dpn1 (specific for methylated DNA), leaving only mutated plasmid DNA. The Dpn1-digested material was transformed into competent *E. coli* DH5α cells and plated on LB agar containing 30 μg/mL Km. Plasmids pACCR-MR187A, pACNB-MR188A, pACNB-MR187/188A, and pACCR-MQ100A, encoding the Arg187→Ala, Arg188→Ala, Arg187→Ala/Arg188→Ala, and Gln100→Ala mutants of sMltB, respectively, were isolated from several resulting colonies and sequenced to ensure that only the desired mutation had been made.

Isolation and Purification of sMltB Derivatives. The transformation of *E. coli* DH5α with the respective plasmids

Table 1: Bacterial Strains and Plasmids Used in This Study

strain or plasmid	genotype or characteristic	reference
strains		
Escherichia coli DH5α	K12 ϕ80d *lacZ*Δ*M*15 endA1 *recA1 hsdR17*($r_k^-m_k^-$)*sup E44 thi-1 gyrA96 relA1*Δ(*lacZYA-argF*) U169F$^-$	Gibco/BRL
BL21(λDE3)	F$^-$ *ompT gal* [*dcm*][*lon*] *hsdS$_B$* ($r_B^-m_B^-$)*gla dcm met* λDE3	Novagen
plasmids		
pNBAC54-1	pet30a(+) derivative containing *mltB* on a *Nde*I/*Xho*I fragment	*14*
pACNB-MR188A	pNBAC54-1 encoding the site-specific replacement of Arg188→Ala	this work
pACCR-MR187/188A	PNBAC54-1 encoding the site-specific double replacements of Arg187→Ala and Arg188→Ala	this work
pACCR-MR187A	pNBAC54-1 derivative encoding the site-specific replacement of Arg187→Ala	this work
pACCR-MQ100A-1	pACNB54-1 derivative encoding the site-specific replacement of Gln100→Ala	this work

and their overexpression were conducted as previously described (*14*). The wt and site-directed derivatives of sMltB were purified to apparent homogeneity as determined by sodium dodecyl sulfide−polyacrylamide gel electrophoresis (SDS−PAGE) by a combination of affinity and cation-exchange chromatographies (*14*).

Zymography. The renaturing SDS−PAGE (zymography) protocol used in this study was similar to that previously described (*21*−*23*). Purified insoluble peptidoglycan was incorporated into 12.5% polyacrylamide gels to a final concentration of 0.1% (wt/vol). Following electrophoresis, separated proteins were renatured in situ by incubating gels in 25 mM sodium phosphate buffer, pH 7.0, containing 10 mM $MgCl_2$ and 0.1% Triton X-100 over an 18 h period with periodic buffer changes. Following incubation, the gels were rinsed briefly in deionized water and then stained with a 1% methylene blue solution. Gels were destained in deionized water until zones of clearing due to lytic activity were visible in the blue-stained background of the gel.

Assay for LT Activity. The specific activity and Michaelis−Menten parameters of purified sMltB and its derivatives were measured using the assay developed by Blackburn and Clarke (*24*). Briefly, sMltB (1.1 μM final concentration) was incubated at 37 °C in the presence of 2.5 mg/mL purified insoluble peptidoglycan suspended in 50 mM sodium acetate buffer, pH 5.8, containing 0.1% Triton X-100 (total reaction volume 250 μL). At appropriate time intervals, samples were flash frozen at −78 °C to halt the reaction. The insoluble peptidoglycan was removed from the thawed samples by centrifugation (18000*g*, 20 min, 4 °C), and the recovered supernatants containing the released and soluble muropeptides were evaporated to dryness. The dried samples were hydrolyzed with 5.8 M HCl for 2 h at 98 °C and then evaporated to dryness. The glucosamine contents of the hydrolyzed samples were measured by high-performance anion-exchange chromatography (HPAEC) with a PA1 pellicular anion-exchange column (4 × 250 mm) (Dionex, CA) with pulsed electrochemical detection (*19*). The affect of pH on enzyme activity was determined by assaying for specific activity using insoluble peptidoglycan in 50 mM sodium acetate buffer, pH 4−6, and 50 mM sodium phosphate buffer, pH 6−8, each containing 0.1% Triton X-100.

The Michaelis−Menten parameters of wt sMltB and its derivatives were determined according to a protocol previously described (*14*, *24*) using concentrations of insoluble peptidoglycan ranging from 7.2 μM to 7.0 mM. Calculations of these peptidoglycan concentrations were based on applying a mass of 939.9 g/mol for the repeating GlcNAc-MurNAc-tetrapeptide subunit. Plots of initial reaction velocities as a function of substrate concentration were analyzed by nonlinear regression using the Microcal Origin 6.0 program and assuming a one-site binding model.

Peptidoglycan Binding Assay. Binding of sMltB and select mutant derivatives to insoluble peptidoglycan was analyzed using a procedure described by Ursinus et al. (*25*) with modifications. *P. aeruginosa* PAO1 peptidoglycan suspended in 50 mM sodium acetate buffer, pH 5.8, containing 0.1% Triton X-100 (buffer A) to a final concentration of 4 mg/mL was sonicated (Heat Systems sonicater, 40% maximal power, 2 min processing) to give a uniform suspension. The peptidoglycan stock solution was then equilibrated on ice for 10 min. For binding reactions, 100 μg samples of the peptidoglycan stock suspensions were mixed with 10 μg of protein, and the total reaction volume was brought to 100 μL with ice-cold buffer A. To account for nonspecific binding to the tubes and manipulative loss of protein, a control substituting buffer A for peptidoglycan was used in the experiment. The reaction mixtures were incubated for 30 min on ice, followed by ultracentrifugation in a Beckman airfuge (133000*g*, 23 °C, 10 min). The supernatants were removed and stored. The pellets of insoluble material (i.e., peptidoglycan or precipitated protein) were washed in 100 μL of buffer A and re-isolated by ultracentrifugation (133000*g*, 23 °C, 10 min), and the supernatants were retained. The insoluble pellets were resuspended in 100 μL of 2% SDS and incubated at room temperature for 1 h to extract the bound protein. The SDS-extracted protein was recovered in the supernatants after ultracentrifugation (133000*g*, 23 °C, 10 min). The resulting peptidoglycan pellets were hydrolyzed in 4 M HCl at 98 °C for 48 and then analyzed for GlcN content to normalize the reactions. The retained supernatants were dried in vacuo and analyzed by Western immunoblot using anti-His monoclonal antibody. Relative intensities of the protein bands were determined on a GS-800 densitometer using the Quantity-One software package (Bio-Rad Laboratories). Values for the percent bound protein were determined relative to enzyme incubated in the absence of insoluble peptidoglycan, while values for percent recovered were calculated from the amount of enzyme extracted after incubation in 2% SDS relative to the amount of protein initially bound to the ligand (viz. percent bound).

Determination of Binding Parameters by SUPREX. The protocols used to generate the H/D denaturation curves were as described previously for sMltB (*15*) and are based on the technique developed by Powell and co-workers (*26*). Briefly, hydrogen/deuterium exchange reactions were initiated by combining 1 μL samples of 8.9 μM sMltB stock solution in 10 mM ammonium acetate buffer, pH 6.5, and 100 mM NaCl

(buffer B) with 9 μL volumes of deuterated exchange buffer (10 mM sodium acetate and 100 mM NaCl in D_2O, pD 6.1) containing concentrations of GdmCl that varied from 0 to 8 M. For protein−ligand interaction studies, 1 μL of the protein solution was combined with 1 μL of 2.7 mM ligand in buffer B and 9 μL exchange buffer and incubated for 15 min at room temperature. After the specified exchange time, the protein was extracted with a C_4 Zip-tip, washed with 1−3 volumes of ice-cold 5% methanol, and eluted with 5 μL of ice-cold sinapinic acid in 65% acetonitrile with 0.1% TFA. The quenched samples (1 μL) were spotted onto the MALDI MS sample plate, or the internal calibrant BSA was added prior to spotting.

Samples were analyzed in a Bruker Reflex III MALDI-TOF mass spectrometer in linear mode using a 337 nm nitrogen laser set to 109−121 μJ output. A total of 100−200 replicate spectra were collected, processed, and analyzed to determine an average change in mass relative to the fully protonated sample (ΔMass) at each GdmCl concentration. The mass of deuterated sMltB was determined with a two-point internal calibration utilizing BSA [M + H] and [M + 2H] as an internal standard. All H/D exchange experiments were performed in duplicate using separate preparations of enzymes. The data were plotted as ΔMass (deuterated mass − fully protonated mass) as a function of GdmCl concentration. A nonlinear least-squares analysis routine was used for curve fitting (MicroCal Origin 5.0), and the transition midpoint of the graph was determined. The free energy of folding (ΔG°_f) and K_D values for wt and sMltB derivatives employed the equations previously described (*15*, *26*).

Other Analytical Methods. SDS−polyacrylamide gels were prepared using the discontinuous buffer system of Laemmli (*27*) and sample buffer containing SDS and 2-mercaptoethanol. Gels were stained with Coomassie Brilliant Blue R-250 as described by Bollag et al. (*28*). Protein concentrations were measured using the Sigma BCA protein assay kit with BSA serving as the standard.

Amino acid sequences were aligned using CLUSTAL W (version 1.82) and then adjusted by hand. Protein modeling of the amino acid sequence of sMltB (P41052), lacking the 17 N-terminal amino acids corresponding to the signal sequence and the lipidated cysteine residue, was achieved using 3D-PSSM (version 2.6.0) (*29*) and the high-resolution three-dimensional structure of *E. coli* Slt35 (1QDR) as the template.

RESULTS

Sequence Alignment and Protein Modeling. A search of the finished and unfinished genome databases at NCBI led to the identification of 46 known and hypothetical amino acid sequences with significant similarity (>20% identity) to the family 3 LT MltB from *P. aeruginosa* (Figure 2). With the increased availability of genome sequences, this analysis thus provided the further identification of 29 new members of this LT family (*12*) and additionally permitted its division into two subfamilies on the basis of the alignments around the putative catalytic acid/base Glu residue (Glu162 in both *E. coli* (*30*, *31*) and *P. aeruginosa* (*18*) MltB's). A number of invariant residues were identified both within the subfamilies and across the entire family of LTs, while others are highly conserved. As reported previously, *P. aeruginosa* MltB shares 72% amino acid sequence identity with its *E. coli* homologue, Slt35 (*12*). With such a high degree of identity, the *P. aeruginosa* can be modeled on the known three-dimensional structure of *E. coli* Slt35 (1QDR) with considerable confidence (*E* value, 8.22×10^{-40}) (Figure 3). The active-site cleft of the enzyme is comprised of four substrate-binding subsites (−2, −1, +1, +2), with the single catalytic Glu162 residue (*E. coli* and *P. aeruginosa* numbering) positioned between subsites −1 and +1 (*30*). Of the 12 residues present in the four binding subsites of Slt35, known to make contacts with peptidoglycan derivatives (Table 2), two are invariant while seven others are highly conserved within the family of sequences (data not shown). Both of the invariant residues, Arg188 and the catalytic Glu162, together with the highly conserved Arg187, are located at subsite −1. By analogy with *E. coli* Slt35, Arg187 and Arg-188 are predicted to interact with the stem peptide on the MurNAc residue at subsite −1 (Figure 3). Gln100 appears to be in position to interact with the *N*-acetyl group on MurNAc and thereby may be responsible for properly orienting the *N*-acetyl group for formation of the putative oxazoline reaction intermediate. However, while present in both *E. coli* Slt35 and *P. aeruginosa* MltB, this residue is not highly conserved within the family 3 LTs (data not shown). Nonetheless, Gln100 and the two Arg residues were targeted for site-directed replacement to investigate their function.

Site-Directed Mutagenesis and Production of sMltB Mutants. Using the plasmid pNBAC54-1 encoding the truncated form of MltB (sMltB) as template, PCR primers were designed to replace the nucleotides corresponding to residues Arg187, Arg188, and Gln100 to alanine. The PCR products were sequenced to confirm the expected sequences and then transformed into *E. coli* DH5α and *E. coli* BL21(MDE3)-(pLysS). The constructs, named pACNB-MR188A, pACCR-MR187A, pACCR-MR187/188A, and pACCR-MQ100A-1, respectively, contained the desired mutations with no additional changes. Overexpression of the genes and purification of the site-directed mutant proteins followed the protocol established for wt sMltB (*14*, *15*). As with wt sMltB, yields of 1.8−7.5 mg of proteins were recovered following their purification by affinity and ion-exchange chromatographies.

Activity of Site-Directed Mutants. Zymogram analysis revealed that the ability of the Arg187Ala and Arg188Ala mutants to solubilize insoluble peptidoglycan was significantly decreased in comparison to that of wt sMltB (Figure 4). This decrease was more prominent with the Arg187Ala mutant protein, and the inhibition was exacerbated in the double mutant with the introduction of the second site-specific replacement at Arg188. In contrast, replacement of Gln100 did not appear to affect activity as judged by zymogram analysis.

In an attempt to obtain more quantitative data on the activity of the sMltB derivatives, their specific activity was determined and compared to that of the wild-type enzyme. Each of the enzymes (2.4 mg/mL) was incubated with insoluble peptidoglycan at pH 5.8 in the presence of 0.1% Triton X-100 (final concentration), and the amount of soluble product released was determined with time. Using this assay, the Arg188Ala sMltB derivative was observed to be 33% less active than the wild-type enzyme (Table 3). Consistent with the zymographic analysis, the Arg187Ala derivative was found to be considerably less active, as its specific activity

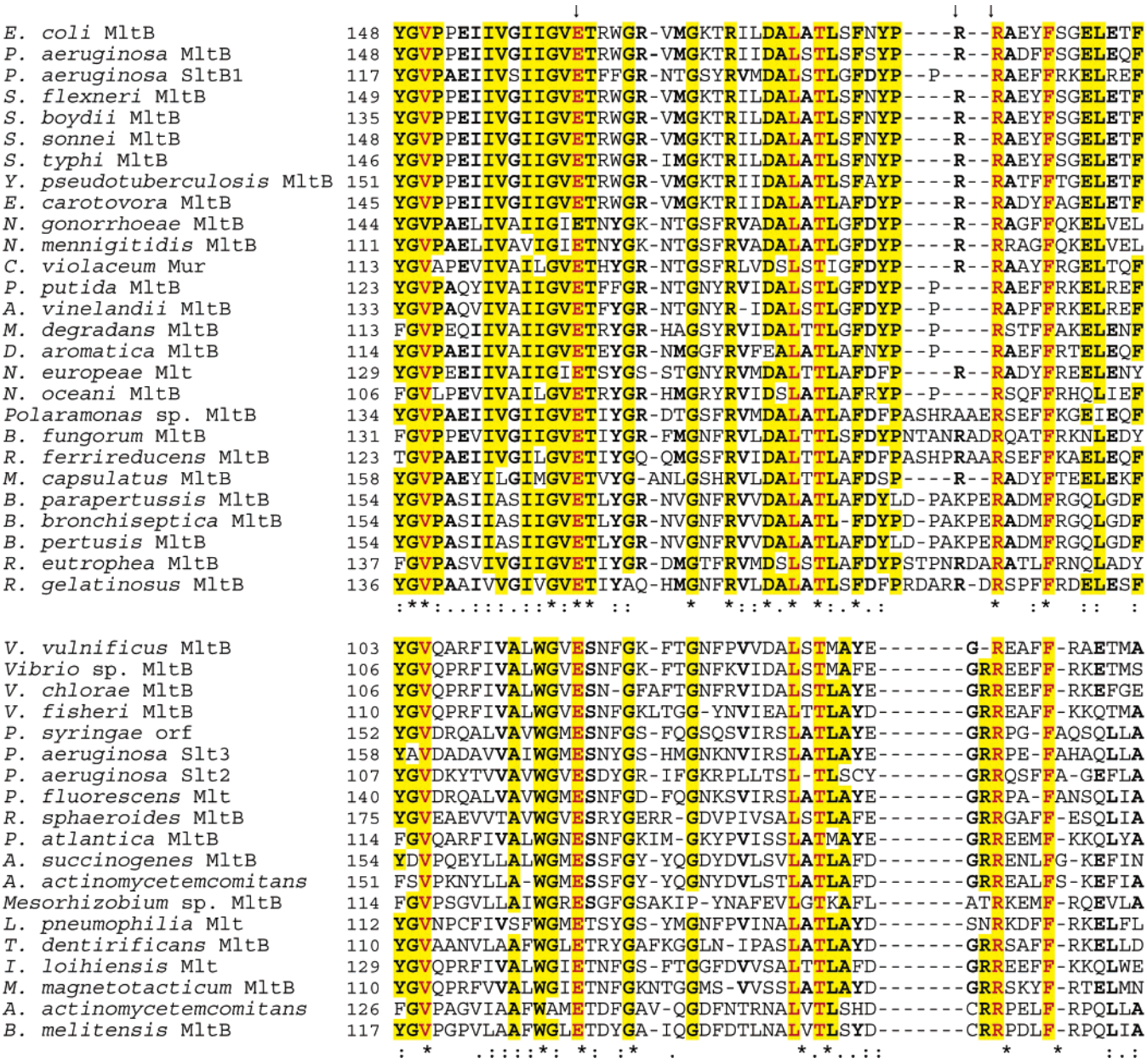

FIGURE 2: Amino acid sequence alignment of the family 3 peptidoglycan lytic transglycosylases. The sequences have been organized into two subfamilies on the basis of alignments around the catalytic Glu residue. Residues in bold and highlighted in yellow denote at least 50% and 80% identity within the two respective subfamilies, while invariant residues across the entire family are in red. The arrows identify the catalytic Glu162 and Arg187, and Arg188 substrate-binding residues. Accession numbers: *E. coli* MltB, P41052; *P. aeruginosa* MltB, g4887205; *P. aeruginosa* SltB1, AAG07388; *S. flexneri* MltB, AAN44216; *S. boydii* MltB, ZP_00696585; *S. sonnei* MltB, YP311685; *S. enterica* MltB, AAV78546; *Y. pseudotuberculosis* MltB, YP071191; *E. carotovora* MltB, CAG73994; *N. gonorrheae* Mur, YP207766; *N. mennigitidis* Mur, CAB84721; *C. violaceum* Mur, AAQ59285; *P. putida* MltB, NP746910; *A. vinelandii* MltB, ZP_00415887; *M. degradans* MltB, ZP_00317854; *D. aromatica* MltB, ZP_00348916; *N. europeae* Mlt, CAD84944, *N. oceani* MltB, YP344617; *Polaramonas* sp. MltB, ZP_00509264; *B. fungorum* MltB, ZP_00281049; *R. ferrireducens* MltB, ZP_00694558; *M. capsulatus* MltB, AAU91882; *B. parapertussis* MltB, NP885296; *B. bronchiseptica* MltB, CAE33951; *B. pertusis* MltB, NP879760; *R. eutrophea* MltB, YP296761; *R. gelatinosus* MltB, ZP_00245110; *V. vulnificus* MltB, NP759141; *Vibrio*. sp. MltB, ZP_00761411; *V. chlorae* MltB, ZP_00760037; *V. fisheri* MltB, YP205085; *P. syringae* orf, AAO58246; *P. aeruginosa* Slt3, ZP_00137432; *P. aeruginosa* Slt2, ZP_00138760; *P. fluorescens* Mlt, AAY94653; *R. sphaeroides* MltB, ABA80843; *P. atlantica* MltB, EAO67942; *A. succinogenes* MltB, EA049636; *A. actinomycetemcomitans* LT, BBA19632; *Mesorhizobium* sp. MltB, ZP_00613770; *L. pneumophilia* Mlt, AAU27946; *T. dentirificans* MltB, ZP334779; *I. loihiensis* Mlt, AAU82656; *M. magnetotacticum* MltB, ZP_00052889; *B. melitensis* MltB, AC3322.

was only 4% of wild-type values. Likewise, the double mutant Arg187Ala/Arg188Ala sMltB possessed minimal specific activity, being 2% of the value for wild-type enzyme. Analysis of the Gln100Ala sMltB derivative demonstrated virtually wild-type levels of activity, further suggesting that this residue is not important for substrate recognition and/or binding.

The dependence of specific activity of the mutant enzymes on pH was determined using sodium acetate (pH 4−6) and sodium phosphate (pH 6−8) buffers. Under these conditions, a plot of activity as a function of pH was bell-shaped for each of the enzymes with maxima centered at pH 5.8. These results were the same as those obtained with the wild-type enzyme, indicating that replacement of each of the residues

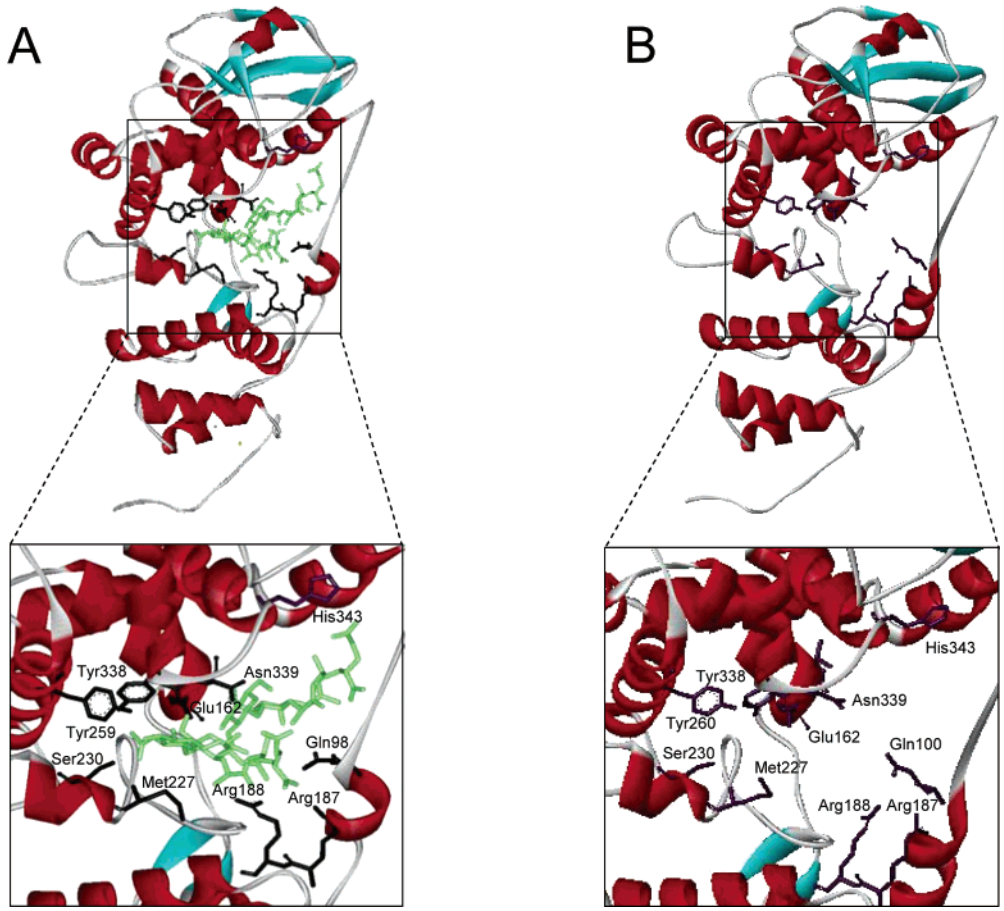

FIGURE 3: Three-dimensional structures of the MltB's from *E. coli* and *P. aeruginosa*. (A) Structure of *E. coli* Slt35 complexed with two molecules of GlcNAc-MurNAc-dipeptide as determined by X-ray diffraction to 1.9 Å resolution (PDB accession number 1DOK). Depicted are the amino acid residues within hydrogen-bonding distance of ligand in the four binding subsites of the active-site cleft of the enzyme. (B) Modeled structure of *P. aeruginosa* MltB using the program 3DSM. The amino acids equivalent to those identified in the substrate-binding subsites of *E. coli* Slt35 are identified.

Table 2: Identification of Amino Acid Residues in the Peptidoglycan-Binding Cleft of *E. coli* Slt35 and *P. aeruginosa* sMltB

binding subsite	identified contacts in Slt35-murodipeptide complex[a]	homologous residue in sMltB[b]
+2	Val161 O- - -O6 MurNAc	**Val161**
	Gln207 Oϵ1- - -O1 MurNAc	Gly207
	His343 Nϵ- - -Oδ D-Glu	**His343**
+1	*Glu162 Oϵ2- - -O3 GlcNAc	***Glu162**
	Asn339 Nδ2- - -O4 GlcNAc	**Asn339**
−1	Gln98 Nϵ2- - -O7 MurNAc	Gln100
	Tyr338 Oη- - -O6 MurNAc	**Tyr338**
	*Glu162 Oϵ2- - -O6 MurNAc	***Glu162**
	Arg187 Nη—CO D-Glu	**Arg187**
	Arg188 Nη- - -O10 MurNAc	**Arg188**
−2	Tyr259 Oη- - -O3 GlcNAc	Tyr260
	Ser230 Oγ- - -O7 GlcNAc	**Ser230**
	Met227 N- - -O7 GlcNAc	**Met227**

[a] Residues within 3.5 Å of muropeptides observed in crystal structure of Slt35-muropeptide complex and proposed to form hydrogen bonds (- - -) or salt bridge (—) (*30*). [b] Residues in bold denote equivalence in both identity and sequence position. The asterisks denote the known catalytic acid/base Glu.

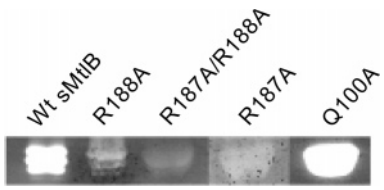

FIGURE 4: Zymogram analysis of wt and mutant derivatives of sMltB with *P. aeruginosa* peptidoglycan as substrate.

Table 3: Specific Activity of Wild-Type and sMltB Derivatives

enzyme	specific activity[a] (nmol GlcN min^{-1} mg^{-1})	ΔActivity (%)
wt	13 ± 4.1[b]	
R187A	0.58 ± 0.02	−96
R188A	4.3 ± 0.09	−67
R187A/R188A	0.22 ± 0.10	−98
Q100A	12 ± 2.9	−5

[a] Enzymes (1.1 μM final concentration) were incubated at 37 °C in the presence of 2.5 mg/mL insoluble peptidoglycan in 50 mM sodium acetate buffer, pH 5.8, containing 0.1% Triton X-100, and reaction products were quantified by HPAEC. [b] Standard deviation (n = 3).

with Ala did not perturb the pK_a's of catalytic groups in the sMltB derivatives.

The Michaelis−Menten parameters for the various sMtlB derivatives at final concentrations of 1.1 μM were determined using insoluble peptidoglycan as substrate in sodium acetate buffer, pH 5.8, and 0.1% Triton X-100 at 23 °C (final substrate concentrations calculated to be 7.2 μM to 7 mM). Under these conditions, the K_M value for the Arg187Ala sMltB was 800-fold higher than that for wild-type enzyme (Table 4), which was anticipated given the activity measurements described above. In addition, this decrease in apparent affinity was compounded by a surprising significant decrease

Table 4: Michaelis−Menten Parameters of sMltB and Arg187Ala and Arg188Ala Derivatives for Insoluble Peptidoglycan

enzyme	K_M[a] (μM)	k_{cat} (s^{-1})	k_{cat}/K_M (s^{-1} M^{-1})	fold decrease
wt[b]	72 ± 20[c]	0.45 ± 0.12	6240	
R187A	1610 ± 64	0.0041 ± 0.0003	2.6	2450
R188A	100 ± 27	0.049 ± 0.003	490	13

[a] Substrate concentrations calculated using the mass of the PG monomeric unit (GlcNAc-MurNAc-tetrapeptide) of 939.9 g mol^{-1}. [b] Values taken from ref *14*. [c] Standard deviation ($n = 3$).

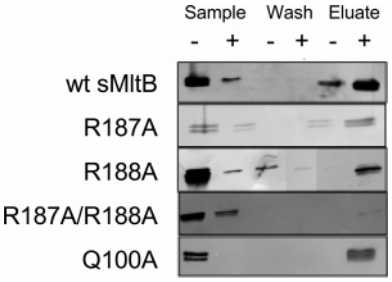

FIGURE 5: Binding affinity of wt and mutant derivatives of sMltB to insoluble peptidoglycan. Sample: Preparations of the various enzymes were incubated (−) in the absence and (+) in the presence of insoluble peptidoglycan in 50 mM sodium acetate buffer, pH 5.8, containing 0.1% Triton X-100 (buffer A) and then subjected to ultracentrifugation. Wash: The pelleted insoluble material was washed with buffer A and resubjected to ultracentrifugation. Eluate: Insoluble pellets were incubated with buffer A containing 2% SDS. For each treatment (i.e., sample, wash, eluate), a sample of the supernatant was analyzed by SDS−PAGE.

in its k_{cat} value, such that the overall efficiency of the sMltB derivative was 2450-fold lower than that of wild-type enzyme, as reflected by k_{cat}/K_M.

The apparent affinity of Arg188Ala sMltB for this substrate was only marginally less than that for the wild-type, but its k_{cat} value was approximately 10-fold less than the wild-type value. The overall effect of these changes resulted in an enzyme derivative that was 13-fold less efficient. Attempts to obtain Michaelis−Menten parameters for the double mutant Arg187Ala/Arg188Ala proved unsuccessful because concentrations of reaction products were below detection limits, even after prolonged incubation times. Unfortunately, scaling up reaction conditions did not help in view of technical difficulties associated with a sparingly soluble enzyme in combination with an insoluble substrate.

Binding Affinity Measurements of sMltB and Its Derivatives. To further investigate the role of the target residues in substrate recognition, the ability of sMltB and its mutant derivatives to bind peptidoglycan was assessed using an affinity assay developed by Ursinus and co-workers (*25*) which takes advantage of the insolubility of the substrate. Thus, Western immunoblot analysis with anti-His_6 antibody was used to detect sMltB and its derivatives (10 μg of each) after their release from 100 μg samples of insoluble peptidoglycan by SDS denaturation following appropriate incubation. These data are presented in Figure 5 and Table 5. Replacement of Arg187 with Ala appeared to have a large effect on the ability of the sMltB to bind its substrate, as only 37% of the enzyme remained associated with the insoluble peptidoglycan after its recovery by centrifugation, compared to values in excess of 90% for the wild-type enzyme. Replacement of Arg188 with Ala also caused a decrease in the ability of sMltB to bind the peptidoglycan substrate, but to a much lesser extent compared to Arg187Ala sMltB. This apparent lesser contribution of Arg188 to peptidoglycan binding is reflected in experiments conducted with the double mutant protein, as only a small difference in binding levels was observed between Arg187Ala/Arg188Ala sMltB and Arg187Ala sMltB. Consistent with the specific activity studies described above, Gln100Ala sMltB was observed to bind to peptidoglycan with the same apparent affinity as wild-type enzyme, thus further indicating that this residue likely does not participate directly in substrate binding.

Table 5: Binding Affinity of Wild-Type sMltB and Its Derivatives for Insoluble Peptidoglycan[a]

enzyme	% bound[b]	% recovered[c]
wt	93 ± 10[d]	64 ± 16
R187A	37 ± 14	71 ± 12
R188A	59 ± 18	95 ± 10
R187/188A	31 ± 12	90 ± 14
Q100A	95 ± 12	85 ± 16

[a] Enzymes (10 μg) were incubated with 100 μg of insoluble peptidoglycan suspended in 50 mM sodium acetate buffer, pH 5.8, containing 0.1% Triton X-100 for 30 min prior to centrifugation to recover enzyme-bound ligand. [b] Calculated on the basis of the amount remaining in the supernatant after incubation with peptidoglycan. [c] Calculated on the basis of the amount bound as 100%. [d] Standard deviation ($n = 3$).

The mutant proteins that showed decreased affinity to peptidoglycan were selected for determination of binding parameters using the MALDI MS-based SUPREX technique. Samples (0.89 μM final concentration) of the site-directed mutant enzymes Arg187Ala, Arg188Ala, and Arg187/188Ala were initially compared to the wt sMltB on the basis of their global unfolding parameters (*15*, *26*). Results with all three sMltB derivatives showed similar denaturation profiles, indicating that the amino acid replacements did not alter significantly the stability of their respective tertiary structures (data not shown). Hence, each of the sMltB derivatives was analyzed for its ability to bind the soluble ligand MurNAc-dipeptide by SUPREX. Under the conditions employed, both Arg187Ala sMltB and Arg187Ala/Arg188Ala sMltB did not demonstrate binding to 0.27 mM MurNAc-dipeptide using this technique. Presumably, the affinity of these two sMltB derivatives for the small ligand was beyond the detection limits of the assay, which is based on protection from denaturation by the chaotropic reagent GdmHCl. However, a K_D value of 2.02 mM was obtained for the binding of this ligand to Arg188Ala sMltB (Table 6). This value represents only a modest 2-fold increase over that of the wild-type enzyme.

DISCUSSION

Our previous characterization of sMltB−ligand interactions using the SUPREX technique indicated that significant binding contributions are made through both the *N*-acetyl and C-3 lactyl moieties of MurNAc, with additional contributions to binding provided by associated peptides (*15*). On the basis of the modeled three-dimensional structure of sMltB, we predicted that Arg187, Arg188, and Gln100, in addition to the catalytic Glu162 (*18*), may figure prominently in these binding interactions at subsite −1. These predictions

Table 6: Binding Constants Obtained by SUPREX for Wild-Type sMltB and Its Derivatives Using MurNAc-Dipeptide as Ligand

enzyme	$C1/2_{SUPREX}$[a] (M)	$\Delta\Delta G_f$[b] (kJ mol^{-1})	K_D (mM)
wt[c]	3.4 ± 0.49[d]	-1.5 ± 0.22	1.1 ± 0.36
R187A	2.3 ± 0.25	nd	
R188A	2.6 ± 0.18	-0.75 ± 0.19	2.0 ± 0.47
R187/188A	2.1 ± 0.24	nd	

[a] All SUPREX experiments were performed using GdmCl as denaturant, with a 15 min exchange time at ambient temperature. [b] Values calculated using ΔG_f values obtained in same manner as in ref *15* (i.e., $\Delta G_{f\ (ligand)} - \Delta G_{f(no\ ligand)}$). [c] Values obtained from ref *15*. [d] Standard deviation of two separate experiments using different preparations of enzyme. nd, not detected.

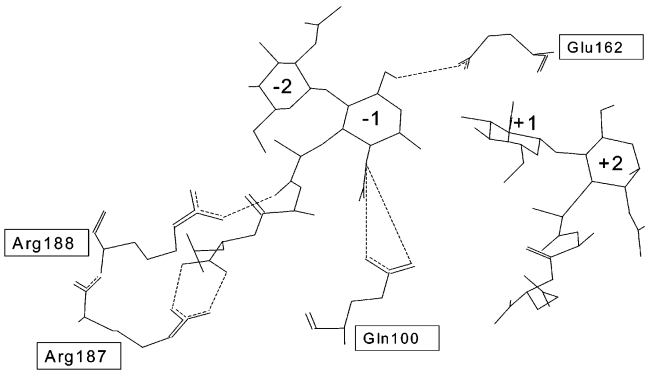

FIGURE 6: Binding interactions at subsite −1 of Slt35 and GlcNAc-MurNAc-dipeptide. The figure is adapted from ref *30*.

were borne out in the current study for the Arg residues. In contrast, the role of Gln100 would appear to be less important. Perhaps this latter finding should not be too surprising, given that Gln100 is not highly conserved among the 46 aligned amino acid sequences of the family 3 LTs; its equivalent is retained by less than half of those analyzed.

Replacement of the each of the Arg residues with Ala affected both binding affinity and activity. These assays indicated that, of these two residues, Arg187 appears to play a more important role. In a complex of the *E. coli* Slt35 with GlcNAc-MurNAc-dipeptide, this residue has been shown to form a salt bridge to the D-Glu of the stem peptide (*30*) (Figure 6), and a similar reaction is likely to occur in an sMtlB complex in view of the high degree of identity between these two enzymes (Figure 2). This conclusion is supported by the facts that both the binding of the Arg187Ala mutant enzyme with insoluble peptidoglycan was reduced by over 60% compared to that of wt sMltB and its K_M value for this substrate was increased by over 22-fold. With the soluble monomeric unit of MurNAc-dipeptide, the binding affinity was reduced to such a low level that it was undetectable by the SUPREX technique. Replacement of Arg188 did not lead to such drastic effects, and a K_D of 2.02 mM was obtained by SUPREX. This represents only a modest 2-fold reduction in the affinity for MurNAc-dipeptide. Likewise, the K_M of this sMltB derivative for insoluble peptidoglycan was only slightly higher compared to that of the wild-type enzyme. These data thus suggest that the interaction between Arg188 and the lactyl carbonyl on MurNAc does contribute to substrate binding but plays a more complementary role compared to the putative salt bridge between Arg187 and the peptidoglycan stem peptide at subsite −1.

The finding that Arg187 appears to play a more dominant role in ligand binding at subsite −1 compared to Arg188 was somewhat surprising, given that only the latter is completely conserved in all examined enzymes, whereas Arg187 is retained in only 70% of the aligned MltB sequences. This situation may reflect the nature of the interactions involving the respective residues. The invariant Arg188 is known to interact with the glycan portion of the peptidoglycan (specifically the lactyl group of muramoyl residues) (*30*), which lacks any heterogeneity in its composition. Thus, this residue appears to be always available to (a) help provide specificity for the enzyme, as the presence of muramic acid is unique to peptidoglycan, and (b) properly orient the glycan backbone of substrate into the binding cleft. On the other hand, heterogeneity does exist at the second position in the stem peptide of peptidoglycans produced by different bacteria, especially with Gram-positives, where the free carboxyl moiety of D-Glu may be amidated or the entire amino acid can be replaced with nonacidic residues (*32*). Such modifications of, or replacements to, the acidic residue would thus preclude the opportunity in these instances to form a salt bridge with Arg187. Although all of the sequences presented in Figure 3 that lack an equivalent to Arg187 are produced by Gram-negative bacteria, it is possible that these specific enzymes do not function on their own cell wall but rather serve as autolysins with a predatory role, as previously demonstrated with *P. aeruginosa* (*33*−*35*) and a number of other bacteria (*35*−*37*). Indeed, it is interesting to note that of the four family 3 LTs encoded by *P. aeruginosa*, the one that lacks an Arg187 equivalent is produced naturally in soluble form as opposed to being membrane bound. Thus, this SltB would be available for such a predatory function against, perhaps specifically, Gram-positive bacteria. An alternative explanation for the presence of only one Arg residue at subsite −1 of some family 3 LTs could involve slight variations in its architecture to permit the formation of a salt bridge or other stronger interactions with substrate involving the invariant Arg188.

In addition to an apparent decrease in affinity, replacement of Arg188 and, to a greater extent, Arg187 with Ala had a significant effect on k_{cat} (viz., 10- and 100-fold decreases, respectively). These decreases were unexpected but clearly indicated an important function for the basic residues in catalysis, in addition to their role in ground-state binding of substrate. Indeed, binding at this subsite involves not only substrate in the ground state but also the stabilization of both the transition state(s) and reaction intermediate. For MltB's, this reaction intermediate has been proposed to be the oxazolium derivative of MurNAc (Figure 1) (*17*, *18*, *30*). The interactions observed in the crystal structure of *E. coli* Slt35 and, by analogy, proposed for *P. aeruginosa* sMltB involve binding of reaction product. However, it would be expected that, during the course of reaction, subtle conformational changes occur that may involve the use of Arg188 and/or Arg187 in the more critical role of stabilizing the oxazolium intermediate. In this regard, an analogous role of an arginyl residue has been proposed for the human hexosaminidase B, a member of the CAZy family 20 glycosidases (*38*). Like the chitinases and LTs, this hexosaminidase is thought to catalyze its reaction by anchimeric assistance involving an oxazolium intermediate. However, Arg211 of the hexosaminidase is proposed to form hydrogen bonds with

both the C-3 and C-4 hydroxyls of glycan at subsite −1, making it positioned appropriately for interactions with the forming oxazolium ring of the reaction intermediate. Binding interactions of Arg187 and Arg188, on the other hand, occur at sites further removed from the glycan backbone. Hence, it would appear that relatively more movement of either of these residues would be required to provide any stabilization of the reaction intermediate.

It is conceivable that substitution of the Arg residues with Ala would disrupt the local environment of the active site and, either directly or indirectly, perturb the pK_a of the neighboring catalytic Glu162. Such a modification would shift the pH optimum of the sMltB derivative's activity and hence be reflected as a decrease in activity when compared to that of wild-type enzyme. However, this possibility was not supported by the observation that the pH optimum of the activity of the Arg187Ala derivative was the same as that of the wt sMltB. Alternatively, the drastic drop in turnover number could be a consequence of the binding of substrate in a nonproductive mode to the enzyme's active site, in view of the heteropolymeric composition of peptidoglycan. This phenomenon has been observed in studies of several other glycosidases, including lysozyme (*39*−*41*). The situation with sMltB would be exacerbated by the fact that its active site is comprised of only four binding subsites (*30*), compared to lysozyme's six (*42*). Thus, diminishing the specificity at subsite −1 for muramoyl residues might have permitted the misalignment of the peptidoglycan substrate in a nonproductive mode. Under such conditions, the k_{cat} would be expected to be decreased, because at saturation only a fraction of the substrate is bound productively. However, the additional binding modes, albeit nonproductive, would also serve to lower the K_M, with the result that the overall k_{cat}/K_M value should remain unaffected (*43*). Clearly, this was not the case for the Arg187Ala and Arg188Ala derivatives.

The nonproductive binding of substrate into the active-site cleft of MltB may indirectly affect catalysis when one considers the mechanism of action postulated for the enzyme. Molecular modeling of Slt35 with peptidoglycan ligands indicated that the stem peptide in the +2 subsite was not as tightly bound as the stem peptide in the −1 subsite. This free stem peptide in the +2 subsite could be modeled such that the free carboxyl of its D-Glu was in position to interact with the MurNAc *N*-acetyl group in the −1 subsite and thereby activate it for nucleophilic attack (*30*). This function for the stem peptide at the +2 subsite was proposed because, unlike both the CAZy family 20 chitinases that employ anchimeric catalysis (*44*, *45*) and the family 1 LT from *E. coli* Slt70 (*46*), MltB does not appear to possess a residue appropriately positioned in the active site to increase the nucleophilicity of the *N*-acetyl carbonyl and thereby facilitate the formation of an oxazolinium intermediate. The critical role of this functionality for glycosidases employing anchimeric assistance has been clearly demonstrated in a study of *Streptomyces plicatus* β-hexosamindase (*47*). The use of the neighboring stem peptide for this purpose is substantiated by the observation that the MltB's from both *E. coli* (*48*) and *P. aeruginosa* (*14*) have an absolute requirement for the stem-peptide portion of peptidoglycan for activity; unlike lysozyme, these LTs are not active on chitin or chitooligosaccharides. Hence, if the stem peptide is serving this catalytic function in MltB, its proper positioning and orientation within the binding cleft would be essential. Given this, the nonproductive binding of peptidoglycan and/or its misalignment into the active site of the enzyme would have a direct inhibitory effect on catalysis.

Our previous studies highlighted the importance of the C-3 lactyl moiety of muramoyl residues and associated peptide for the binding of small soluble ligands to sMltB, while the presence of GlcNAc as a component of a disaccharide ligand provided only a modest enhancement. The results of the current study confirm this finding and furthermore demonstrate the importance of interactions specifically at subsite −1 for productive binding and activity. This is consistent with the activity of MltB's as exo-acting enzymes catalyzing the release of GlcNAc-1,6-anhydroMurNAc-peptides from the ends of peptidoglycan chains. As such, the terminal disaccharide-peptide of the glycan chain bound at subsites +1 and +2 would need to diffuse readily from the enzyme upon cleavage, suggesting that the binding interactions at these subsites would have to be weaker than those at subsites −1 and −2. That the binding-site cleft of MltB can accommodate a total of only four glycan residues further underscores the importance for the network of binding interactions at subsite −1, which can exploit the opportunities provided by both glycan and peptide. This finding may prove important for the development of a specific and efficient inhibitor of the LTs. Indeed, our previous studies with NAG-thiazoline (*17*, *18*), a potent inhibitor of the family 20 glycosidases (*44*, and references therein), showed that it only weakly inhibits the family 3 LTs. NAG-thiazoline is a derivative of GlcNAc and mimics structurally the postulated oxazoline reaction intermediate that would exist in subsite −1. The results of the current study would suggest that enhancement of binding affinity to generate a more powerful inhibitor would require at minimum the presence of the lactyl moiety at C-3 of the glucosamine to produce a muramoyl derivative. Unfortunately, our efforts to date to synthesize thiazoline derivatives of muramic acid have failed due to the instability of synthetic intermediates.

ACKNOWLEDGMENT

We thank Dr. Dyanne Brewer, Biological Mass Spectrometry Facility, University of Guelph, for her expert technical assistance with MALDI-TOF MS.

REFERENCES

1. Young, K. D. (2003) Bacterial shape, *Mol. Microbiol. 49*, 571−580.
2. Ghyusen, J.-M., and Hakenbeck, R. (1994) *Bacterial cell wall*, Elsevier, Amsterdam.
3. Holtje, J. V. (1998) Growth of the stress-bearing and shape-maintaining murein sacculus of *Escherichia coli*, *Microbiol. Mol. Biol. Rev. 62*, 181−203.
4. Holtje, J. V., Mirelman, D., Sharon, N., and Schwarz, U. (1975) Novel type of murein transglycosylase in *Escherichia coli*, *J. Bacteriol. 124*, 1067−1076.
5. Goodell, E. W. (1985) Recycling of murein by *Escherichia coli*, *J. Bacteriol. 163*, 305−310.
6. Holtje, J. V., and Tuomanen, E. I. (1991) The murein hydrolases of *Escherichia coli*: properties, functions and impact on the course of infections *in vivo*, *J. Gen. Microbiol. 137*, 441−454.
7. Koraimann, G. (2003) Lytic transglycosylases in macromolecular transport systems of Gram-negative bacteria, *Cell. Mol. Life Sci. 60*, 2371−2388.

8. Dijkstra, A. J., and Keck, W. (1996) Peptidoglycan as a barrier to transenvelope transport, *J. Bacteriol. 178*, 5555−5562.
9. Clarke, A. J., and Dupont, C. (1992) *O*-Acetylated peptidoglycan: its occurrence, pathobiological significance, and biosynthesis, *Can. J. Microbiol. 38*, 85−91.
10. Luker, K. E., Collier, J. L., Kolodziej, E. W., Marshall, G. R., and Goldman, W. E. (1993) *Bordetella pertussis* tracheal cytotoxin and other muramyl peptides: distinct structure−activity relationships for respiratory epithelial cytopathology, *Proc. Natl. Acad. Sci. U.S.A. 90*, 2365−2359.
11. Melly, M. A., McGee, Z. A., and Rosenthal, R. S. (1984) Ability of monomeric peptidoglycan fragments from *Neisseria gonorrhoeae* to damage human fallopian-tube mucosa, *J. Infect. Dis. 149*, 378−386.
12. Blackburn, N. T., and Clarke, A. J. (2001) Identification of four families of peptidoglycan lytic transglycosylases, *J. Mol. Evol. 52*, 78−84.
13. Govan, J. R., and Deretic, V. (1996) Microbial pathogenesis in cystic fibrosis: mucoid *Pseudomonas aeruginosa* and *Burkholderia cepacia*, *Microbiol. Rev. 60*, 539−574.
14. Blackburn, N. T., and Clarke, A. J. (2002) Characterization of soluble and membrane-bound family 3 lytic transglycosylases from *Pseudomonas aeruginosa*, *Biochemistry 41*, 1001−1013.
15. Reid, C. W., Brewer, D., and Clarke, A. J. (2004) Substrate binding affinity of *Pseudomonas aeruginosa* membrane-bound lytic transglycosylase B by hydrogen−deuterium exchange MALDI MS, *Biochemistry 43*, 11275−11282.
16. Knapp, S., Vocadlo, D. J., Gao, Z., Kirk, B., Lou, J., and Withers, S. G. (1996) NAG-thiazoline, an *N*-acetyl-betahexosaminidase inhibitor that implicates acetamido participation, *J. Am. Chem. Soc. 118*, 6804−6805.
17. Reid, C. W., Blackburn, N. T., and Clarke, A. J. (2004) The effect of NAG-thiazoline on morphology and surface hydrophobicity of *Escherichia coli*, *FEMS Microbiol. Lett. 234*, 343−348.
18. Reid, C. W., Blackburn, N. T., Legaree, B. A., Auzanneau, F. I., and Clarke, A. J. (2004) Inhibition of membrane-bound lytic transglycosylase B by NAG-thiazoline, *FEBS Lett. 574*, 73−79.
19. Clarke, A. J. (1993) Compositional analysis of peptidoglycan by high-performance anion-exchange chromatography, *Anal. Biochem. 212*, 344−350.
20. Glauner, B. (1988) Separation and quantification of muropeptides with high-performance liquid chromatography, *Anal. Biochem. 172*, 451−464.
21. Bernadsky, G., Beveridge, T. J., and Clarke, A. J. (1994) Analysis of the sodium dodecyl sulfate-stable peptidoglycan autolysins of select gram-negative pathogens by using renaturing polyacrylamide gel electrophoresis, *J. Bacteriol. 176*, 5225−5232.
22. Watt, S. R., and Clarke, A. J. (1994) Role of autolysins in the EDTA-induced lysis of *Pseudomonas aeruginosa*, *FEMS Microbiol. Lett. 124*, 113−119.
23. Watt, S. R., and Clarke, A. J. (1997) Isolation, purification, and characterization of the major autolysin from *Pseudomonas aeruginosa*, *Can. J. Microbiol. 43*, 1054−1062.
24. Blackburn, N. T., and Clarke, A. J. (2000) Assay for lytic transglycosylases: a family of peptidoglycan lyases, *Anal. Biochem. 284*, 388−393.
25. Ursinus, A., van den Ent, F., Brechtel, S., de Pedro, M., Holtje, J. V., Lowe, J., and Vollmer, W. (2004) Murein (peptidoglycan) binding property of the essential cell division protein FtsN from *Escherichia coli*, *J. Bacteriol. 186*, 6728−6737.
26. Powell, K. D., Ghaemmaghami, S., Wang, M. Z., Ma, L., Oas, T. G., and Fitzgerald, M. C. (2002) A general mass spectrometry-based assay for the quantitation of protein−ligand binding interactions in solution, *J. Am. Chem. Soc. 124*, 10256−10257.
27. Laemmli, U. K. (1970) Cleavage of structural proteins during the assembly of bacteriophages T4, *Nature 227*, 680−685.
28. Bollag, M., Rozycki, M. D., and Edelstein, S. J. (1996) *Protein Methods*, pp 499−520, Wiley-Liss, Toronto.
29. Kelly, L. A., MacCallum, R. M., and Sternberg, M. J. E. (2000) Enhanced genome annotation using structural profiles in the program 3D-PSSM, *J. Mol. Biol. 299*, 499−520.
30. van Asselt, E. J., Kalk, K. H., and Dijkstra, B. W. (2000) Crystallographic studies of the interactions of *Escherichia coli* lytic transglycosylase Slt35 with peptidoglycan, *Biochemistry 39*, 1924−1934.
31. van Asselt, E.J., Dijkstra, A. J., Kalk, K. H., Takacs, B., Keck, W., and Dijkstra, B. W. (1999) Crystal structure of *Escherichia coli* lytic transglycosylase Slt35 reveals a lysozyme-like catalytic domain with an EF-hand, *Structure 7*, 1167−1180.
32. Schleifer, K. H., and Kandler, O. (1972) Peptidoglycan types of bacterial cell walls and their taxonomic implications, *Bacteriol. Rev. 36*, 407−477.
33. Kadurugamuwa, J. L., and Beveridge, T. J. (1996) Bacteriolytic effect of membrane vesicles from *Pseudomonas aeruginosa* on other bacteria including pathogens: conceptually new antibiotics, *J. Bacteriol. 178*, 2767−2774.
34. Kadurugamuwa, J. L., and Beveridge, T. J. (1997) Natural release of virulence factors in membrane vesicles by *Pseudomonas aeruginosa* and the effect of aminoglycoside antibiotics on their release, *J. Antimicrob. Chemother. 40*, 615−621.
35. Kadurugamuwa, J. L., and Beveridge, T. J. (1999) Membrane vesicles derived from *Pseudomonas aeruginosa* and *Shigella flexneri* can be integrated into the surfaces of other gram-negative bacteria, *Microbiology 145*, 2051−2060.
36. Li, Z., Clarke, A. J., and Beveridge, T. J. (1998) Gram-negative bacteria produce membrane vesicles which are capable of killing other bacteria, *J. Bacteriol. 180*, 5478−5483.
37. Kadurugamuwa, J. L., Mayer, A., Messner, P., Sara, M,. Sleytr, U. B., and Beveridge, T, J. (1998) S-layered *Aneurinibacillus* and *Bacillus* spp. are susceptible to the lytic action of *Pseudomonas aeruginosa* membrane vesicles, *J. Bacteriol. 180*, 2306−2311.
38. Hou, Y., Vocadlo, D., Withers, S., and Mahuran, D. (2000) Role of beta Arg211 in the active site of human beta-hexosamindase B, *Biochemistry 39*, 6219−6227.
39. Yue, Z., Bin, W., Baixu, Y., and Peiji, G. (2004) Mechanism of cellobiose inhibition in cellulose hydrolysis by cellobiohydrolase, *Sci. China C. Life Sci. 47*, 18−24.
40. Kristiansen, A., Varum, K. M., and Grasdalen, H. (1998) Quantitative studies of the non-productive binding of lysozyme to partially *N*-acetylated chitosans. Binding of large ligands to a one-dimensional binary lattice studied by a modified McGhee and von Hippel model, *Biochim. Biophys. Acta 1425*, 137−150.
41. Holler, E., Rupley, J. A., and Hess, G. P. (1975) Productive and unproductive lysozyme-chitosaccharide complexes. Kinetic investigations, *Biochemistry 14*, 2377−2385.
42. Blake, C. C., Johnson, L. N., Mair, G. A., North, A. C., Phillips, D. C., and Sarma, V. R. (1967) Crystallographic studies of the activity of hen egg-white lysozyme, *Proc. R. Soc. London B Biol. Sci. 167*, 378−388.
43. Fersht, A. (1999) *Structure and mechanism in protein science: a guide to enzyme catalysis and protein folding*, 2nd ed., W. H. Freeman and Co., New York.
44. Mark, B. L., Vocadlo, D. J., Knapp, S., Triggs-Raine, B. L., Withers, S. G., and James, M. N. (2001) Crystallographic evidence for substrate-assisted catalysis in a bacterial β-hexosaminidase, *J. Biol. Chem. 276*, 10330−10337.
45. Williams, S. J., Mark, B. L., Vocadlo, D. J., James, M. N., and Withers, S. G. (2002) Aspartate 313 in the *Streptomyces plicatus* hexosaminidase plays a critical role in substrate-assisted catalysis by orienting the 2-acetamido group and stabilizing the transition state, *J. Biol. Chem. 277*, 40055−40065.
46. van Asselt, E. J., Thunnissen, A. M., Dijkstra, B. W. (1999) High-resolution crystal structures of the *Escherichia coli* lytic transglycosylase Slt70 and its complex with a peptidoglycan fragment, *J. Mol. Biol. 291*, 877−898.
47. Williams, S. J., Mark, B. L., Vocadlo, D. J., James, M. N. G., and Withers, S. G. (2002) Aspartate 313 in the *Streptomyces plicatus* beta-hexosaminidase plays a critical role in substrate-assisted catalysis by orienting the 2-acetamido group and stabilizing the transition state, *J. Biol. Chem. 277*, 40055−40065.
48. Romeis, T., Vollmer, W., and Höltje, J.-V. (1993) Characterization of three different lytic transglycosylases from *Escherichia coli*, *FEMS Microbiol. Lett. 111*, 141−146.

BI052342T